THE JOURNAL OF BIOLOGICAL CHEMISTRY VOL. 288, NO. 28, pp. 20267–20279, July 12, 2013

Cytoplasmic Degradation of the *Arabidopsis* Transcription Factor ABSCISIC ACID INSENSITIVE 5 Is Mediated by the RING-type E3 Ligase KEEP ON GOING*[S]

Received for publication, February 28, 2013, and in revised form, May 24, 2013 Published, JBC Papers in Press, May 29, 2013, DOI 10.1074/jbc.M113.465369

Hongxia Liu and Sophia L. Stone[1]

From the Department of Biology, Dalhousie University, Halifax, Nova Scotia B3H 4R2, Canada

Background: KEEP ON GOING (KEG) is required to maintain low levels of the nuclear-localized transcription factor ABI5.
Results: KEG-mediated degradation of ABI5 occurs in the cytoplasm/trans-Golgi network/early endosome and requires a C-terminal lysine residue.
Conclusion: Cytoplasmic degradation prevents nuclear accumulation of ABI5 so as to prohibit ABA signaling.
Significance: Knowing how ABI5 stability is controlled is crucial to understanding ABA signaling and plant survival of environmental stress.

To mitigate the effects of environmental stress the abscisic acid (ABA)-responsive transcription factor ABI5 is required to delay growth of germinated seedlings. In the absence of stress, KEEP ON GOING (KEG) E3 is required to maintain low levels of ABI5. However, the mechanism underlying KEG-dependent turnover of ABI5 is not known. In addition, localization studies place KEG at the trans-Golgi network, whereas ABI5 is nuclear. Here we show that KEG interacts directly with ABI5 via its conserved C3 region. Interactions between KEG and ABI5 were observed in the cytoplasm and trans-Golgi network only when the RING domain of KEG was inactivated or when ABI5 was stabilized via mutations. Deletion of the C-terminal region of ABI5 or substituting lysine 344 for alanine (K344A) prohibited protein turnover. Furthermore, ABI5 is observed in the cytoplasm of *Arabidopsis thaliana* root cells when the K344A mutation is combined with the deletion of a nuclear localization signal. Other lysine mutations (K353A, K364A, and K376A) in conjunction with the nuclear localization signal deletion did not result in cytoplasmic accumulation of ABI5. Loss of lysine 344 did not affect the ability of ABI5 to promote ABA responses, which demonstrates that the mutant transcription factor is still functional. Based on the results, a model is suggested where KEG targets ABI5 for degradation in the cytoplasm, thus reducing nuclear accumulation of the transcription factor in the absence of ABA.

Ubiquitination is responsible for marking regulatory and abnormal proteins for degradation by the 26 S proteasome. The selective removal of specific targets via the covalent attachment of ubiquitin molecules represents an efficient and rapid strategy to control many cellular processes such as response to external stimuli, cell growth, and division. Formation of ubiquitin conjugates on a specific protein requires the sequential action of three enzymes, E1 (ubiquitin activating), which activates ubiquitin molecules forming an E1-ubiquitin intermediate; E2 (ubiquitin conjugating), which accepts the activated ubiquitin from the E1 forming an E2-ubiquitin intermediate; and E3 (ubiquitin ligase), which facilitates the transfer of ubiquitin from the E2-ubiquitin intermediate to the target protein. Ubiquitination of a specific substrate is mainly regulated through modulation of its degradation signal (degron) and through control of the activity of its cognate E3. The E3-dependent recognition of the various primary degradation signals leads to the enzymatic addition of a polyubiquitin chain that serves as a secondary signal for targeting of the substrates to the proteasome (1–3).

Ubiquitin is usually attached via an isopeptide bond to an internal lysine on the substrate. Most target proteins have multiple lysine residues, but only one or a few can be efficiently ubiquitinated. This implies that for these substrates, the position of the ubiquitin acceptor site or the local structure surrounding it serves as a determinant for degron function. The molecular basis for the specificity of a E3 ligase toward a particular lysine in a substrate is poorly understood. Structural studies suggest that specificity can be explained by the relative spatial relationship of the lysine to the E3 ligase (4, 5).

ABSCISIC ACID INSENSITIVE 5 (ABI5),[2] a member of the *Arabidopsis thaliana* (*Arabidopsis*) basic leucine zipper (bZIP) transcription factor family, has been shown to play an important role in controlling abscisic acid (ABA)-dependent postgerminative growth arrest as well as late phases of seed maturation (6, 7). The efficiency of the ABA-induced growth arrest is dependent on ABI5 protein accumulation through transcriptional activation and enhanced protein stability (7, 8). ABI5 protein accumulates in seedlings treated with 26 S proteasome inhibitors and in *RPN10* (a subunit of the 26 S proteasome)

* This work was supported in part by a Natural Science and Engineering Research Council of Canada grant and Human Frontier Science Program Center Developmental Award (to S. L. S.).
[S] This article contains supplemental Table 1.
[1] To whom correspondence should be addressed. Tel.: 902-494-4541; Fax: 902-494-3736; E-mail: sophia.stone@dal.ca.

[2] The abbreviations used are: ABI5, abscisic acid insensitive 5; bZIP, basic leucine zipper; ABA, abscisic acid; KEG, KEEP ON GOING; NLS, nuclear localization signal; RING, really interesting new gene; TGN/EE, trans-Golgi network/early endosome; YC, carboxyl-terminal fragment of enhanced yellow fluorescence protein; YN, amino-terminal fragment of enhanced yellow fluorescence protein; AD, activation domain; BD, binding domain; nt, nucleotide; BiFC, bimolecular fluorescence complementation.

mutant plants, suggesting that ABI5 turnover is dependent on the 26 S proteasome pathway (7, 9). A number of E3 ligases have been shown to be involved in modulating ABI5 stability (10). KEEP ON GOING (KEG), a multidomain really interesting new gene (RING)-type E3 ligase, is required to maintain low levels of ABI5 in the absence of the hormone. This is based on the fact that *keg* mutants undergo growth arrest immediately after germination, accumulate extremely high levels of ABI5, and display hypersensitivity to ABA, whereas overexpression of *KEG* leads to ABA insensitivity (11, 12). Furthermore, complementation studies demonstrate that KEG containing a nonfunctional E3 ligase domain is not able to rescue the *keg-1* phenotype, whereas an intact KEG is able to fully rescue the *KEG* mutant and restore the levels of ABI5 to that observed for wild type plants (12). In addition, KEG is capable of attaching ubiquitin to ABI5 in biochemical assays. Overall, these studies demonstrate that KEG negatively regulates ABI5 abundance to prohibit activation of ABA responses in the absence of the hormone or stress stimulus.

Although KEG has been clearly demonstrated to negatively regulate the abundance of ABI5, the ability of KEG to directly interact with and mediate the turnover ABI5 is inconsistent with previously described cellular localization patterns of ABI5 and KEG. Recent reports suggest that KEG localizes to the trans-Golgi network/early endosome (TGN/EE) vesicles of transiently transformed tobacco epidermal cells (13). This is in contrast to ABI5, which has been shown to be constitutively localized in the nucleus via the use of a promoter-*β-glucuronidases* reporter system (14). Under the control of the cauliflower mosaic virus 35S promoter, ABI5 was only observed in the nucleus of both transiently transformed *Arabidopsis* and onion epidermal cells (15). In light of the apparent spatial separation of the E3 ligase and substrate, the outstanding question of how KEG directly regulates ABI5 turnover remains to be addressed. Here we show that KEG interacts directly with ABI5 in the cytoplasm and TGN/EE via ABI5 conserved C3 region. ABI5 mutations that prohibit KEG-mediated turnover lead to the stabilization and accumulation of ABI5 in the cytoplasm. Overall our results suggest a model where in the absence of ABA, KEG targets ABI5 for degradation in the cytoplasm to maintain low levels of the transcription factor.

EXPERIMENTAL PROCEDURES

Sequence Analysis and Alignment—To identify potential nuclear localization and export signal, the complete amino acid sequence of ABI5 was examined by using the WoLF PSORT computer program (16). Alignments were generated with the ClustalX program (17) and revised using the Se-Al sequence editor (Evolutionary Biology Group, University of Oxford).

Cloning and Mutagenesis—The full-length wild type *KEG* (11), the RING domain mutant of *KEG* (KEG^{AA}; C29A, H31A), and the *ABI5* cDNAs in the gateway entry vector pDONR201 (Invitrogen) were obtained as previously described (12). To be used for C-terminal fusion expression, these cDNAs were amplified again using Phusion polymerase (Finnzymes) to remove the STOP codon and introduced back into pDONR201 as per the manufacturer's instructions. The partial cDNA regions of *KEG* encoding the RING, kinase domain, and ankyrin repeats (KEG^{1-829}; 1–2487 nucleotides (nt)), the RING and kinase domain (KEG^{1-442}; 1–1326 nt), and the ankyrin repeats ($KEG^{497-829}$; 1489–2487 nt) were introduced into pDONR201 as per the manufacturer's instructions. Deletion mutants and point mutations of *ABI5* were generated using the Phusion site-directed mutagenesis kit (Finnzymes). Primers used for making these mutants are listed under supplemental Table S1. Nucleotide sequences were confirmed by DNA sequencing (McGill University and Génome Québec Innovation Centre).

Yeast Two-hybrid Assay—Gateway-compatible vectors pGBKT7-DEST (bait) and pGADT7-DEST (prey) modified from the pGBKT7 and pGADT7-Rec vectors, respectively, were gifts from Dr. Yuhai Cui (Agriculture and Agri-Food Canada, London, ON). The full-length open reading frame of *KEG* as well as KEG^{1-829}, KEG^{1-442}, and $KEG^{497-829}$ were introduced into the activation domain vector pGADT7-DEST. The full-length open reading frames of *ABI5*, deletion mutants, and point mutations of *ABI5* were cloned into the DNA-binding domain vector pGBKT7-DEST. Both bait and prey constructs were co-transformed into yeast strain AH109 using the lithium acetate method according to the manufacturer's instructions (Clontech). Transformants were selected for on medium lacking tryptophan and leucine (SD/-Trp/-Leu). To select for interactions, equal amounts of diluted AH109 carrying the bait and prey constructs was spotted onto selective medium lacking tryptophan, leucine, histidine, and adenine (SD/-Trp/-Leu/-His/-Ade) and incubated at 28 °C for up to 5 days. Empty pGBKT7 and pGADT7-Rec vectors were used as negative controls.

Plant Material and Growth Conditions—*Arabidopsis* ecotype Columbia-0 (Col-0) wild type, mutant, and transgenic seeds were surface-sterilized with 50% (v/v) bleach and 0.1% Triton X-100. After cold treatment at 4 °C for 48 h, seeds were germinated and grown solid on 0.5× Murashige and Skoog (MS) medium containing 0.8% agar and 1% sucrose under continuous light at 22 °C. For plants grown in soil, 7-day-old seedlings were transferred from MS medium to soil and grown under photoperiodic cycles of 16 h light and 8 h dark at 22 °C in a growth chamber. *keg-1* (Salk_049542) seeds obtained from the Arabidopsis Biological Resource Center (ABRC) (19) were a gift from the laboratory of Dr. Judy Callis (University of California, Davis, CA (11)).

Transient Protein Expression in Nicotiana benthamiana—Five-week-old *N. benthamiana* (tobacco) plants used for transient protein expression were grown under a photoperiod of 16 h light and 8 h dark at 23 °C. *Agrobacterium tumefaciens* (*Agrobacterium*) strain GV3101 transformed with the appropriate binary plasmids were grown and prepared for transient expression as described previously (20). *Agrobacterium* cultures were resuspended in infiltration solution (5 mg/ml of D-glucose, 50 mM MES, 2 mM Na_3PO_4, 0.1 mM acetosyringone) at an optical density at 600 nm of 0.8. For co-expression of multiple constructs, suspensions were mixed in equal ratios. *Agrobacterium* suspension mixtures were infiltrated using a needleless syringe into leaves of 5-week-old tobacco plants. Forty-eight hours after *Agrobacterium* infiltration, samples were collected for protein extraction and microscopic imaging.

For proteasome inhibitor treatments, tobacco leaves were injected with 50 μM MG132 32 h after *Agrobacterium* infiltration, excised, and incubated in 50 μM MG132 for another 16 h.

Subcellular Localization and Bimolecular Fluorescence Complementation (BiFC) Assay—For subcellular localization, *KEG* and *KEG*^{AA} cDNAs in the entry vector pDONR201 were introduced into the pEarleyGate101 plant transformation vector (21) using Gateway cloning (Invitrogen) to produce in-frame fusions with the C-terminal yellow fluorescence protein (YFP) and hemagglutinin (HA) tag (KEG-YFP) under the control of the cauliflower mosaic virus ^{35}S promoter. Similarly, full-length *ABI5*, deletion mutants, and point mutations of *ABI5* were cloned into the pEarleyGate102 vector to generate the C-terminal-tagged cyan fluorescent protein (CFP) and HA fusions (ABI5-CFP). For simplification, the HA tag was not included in the names of the fusion proteins throughout the text. Constructs were then introduced into *Agrobacterium* strain GV3101 and transformed into *Arabidopsis* using the flower-dipping method (22) or infiltrated into tobacco leaves as described above.

BiFC vectors pEarleyagte201-YN, containing the N-terminal portion (1–174 amino acids) of enhanced YFP (eYFP) and a HA tag and pEarleygate202-YC containing the C-terminal portion (175–239 amino acids) of eYFP and a FLAG tag were created based on the Gateway-compatible vectors pEarleygate201 and pEarleygate202, respectively, by the laboratory of Dr. Yuhai Cui (Agriculture and Agri-Food Canada, London, United Kingdom (18)). *KEG* and *ABI5* (including deletions and point mutations) cDNAs in the gateway entry vector pDONR201 were recombined into pEarleygate201-YN and pEarleygate202-YC, respectively (Invitrogen). *KEG* is expressed as a fusion with the N-terminal portion of eYFP and a HA tag (KEG-YN). *ABI5* is expressed as a fusion with the C-terminal portion of eYFP and a FLAG tag (ABI5-YC). For simplification, the HA and FLAG tags were not included in the names of the fusion proteins throughout the text. Each plasmid DNA was transformed into *Agrobacterium* strain GV3101. Equal volumes of *Agrobacterium* cultures with cDNAs in the pEarleygate201-YN and pEarleygate202-YC vectors were mixed and used for infiltrating tobacco leaves as described above. Leaves were assayed for fluorescence 48 h after infiltration for both subcellular localization and BiFC assay. Each localization experiment and BiFC assay was repeated at least three times.

Fluorescence Microscopy—Roots of 7-day-old transgenic *Arabidopsis* seedlings or pieces of infiltrated tobacco leaves excised 48 h after infiltration were imaged using a Zeiss LSM 510 META inverted confocal laser scanning microscope (Carl Zeiss MicroImaging GmbH) equipped with a ×25 oil immersion objective. YFP fluorescence was detected at an excitation wavelength of 514 nm, and emissions were collected between 530 and 600 nm. For CFP fluorescence, an excitation wavelength of 458 nm was used, and emissions were collected between 475 and 525 nm. To show the outline of each epidermal cell, a single slice of the fluorescence and bright-field images were overlaid. For those images showing only fluorescence, a series of *Z*-stack images were collected and then combined and processed using the Zeiss LSM Image Browser (Carl Zeiss MicroImaging GmbH).

Protein Extraction and Immunoblot Analysis—Forty-eight hours after *Agrobacterium* infiltration, tobacco leaf discs were collected from the same leaf used for microscopic imaging (see above), frozen in liquid nitrogen, and stored at −80 °C until needed. At least three independent repetitions were performed for each experiment. Total protein was extracted from tissues in protein extraction buffer (HEPES, pH 7.5, 5 mM EDTA, 5 mM EGTA, 10 mM Na_3VO_4, 10 mM NaF, 50 mM β-glycerophosphate, 10 mM dithiothreitol, 1 mM phenylmethylsulfonyl fluoride, 5% glycerol and protease inhibitor mixture (Sigma)). The concentration of protein was determined using the Bradford reagent (Sigma) with bovine serum albumin as a standard. Total protein was mixed with 6× SDS loading buffer (300 mM Tris-HCl, pH 6.8, 30% glycerol, 12% SDS, 0.6% bromphenol blue) boiled for 5 min before loading on SDS-polyacrylamide gel (SDS-PAGE).

For immunoblot analysis, 30 μg of total protein per lane was separated on SDS-PAGE. After electrophoresis, proteins were electrotransferred to polyvinylidene fluoride (PVDF) membrane. After blocking for 1 h in TBST (50 mM Tris-HCl, pH 7.5, 150 mM NaCl, and 0.05% Tween 20) with 5% nonfat dry milk at room temperature, membranes were incubated with mouse anti-FLAG (Sigma) or anti-HA (Sigma) at 1:10,000 dilution for 2 h. Following three washes with TBST, membranes were incubated with horseradish peroxidase-conjugated goat anti-mouse (Sigma) at 1:5000 dilution. After three washes with TBST, the membranes were visualized using an enhanced Lumi-Light Western blotting Substrate kit (Thermo Scientific) following the manufacturer's instructions.

Cell-free Degradation Assay—For recombinant proteins used in the assay, wild type and mutated *ABI5* cDNAs were recombined into modified pDEST527 vectors (Addgene plasmid 11518; donated by Dominic Esposito, National Cancer Institute, Frederick, MD) to obtain fusion proteins with N-terminal FLAG-His tag (12). Recombinant proteins were expressed in *Escherichia coli* strain Rosetta (DE3) and purified using nickel-charged resin (Bio-Rad) according to the manufacturer's protocols.

Cell-free degradation assays were carried out as previously described (23). Total protein was extracted from 4-day-old Col-0 or 8-day-old *keg-1* seedlings using extraction buffer (25 mM Tris-HCl, pH 7.5, 10 mM $MgCl_2$, 5 mM DTT, and protease inhibitor mixture). After centrifugation at 18,000 × *g* for 20 min at 4 °C, the supernatant was transferred to a new tube and the protein concentration was determined using the Bio-Rad protein assay kit. For the degradation assay, 1.6 μg of each recombinant ABI5 protein was incubated in 0.5 mg of total protein extract. $MgCl_2$ (10 mM) and ATP (10 mM) were added to the reaction prior to incubation at 30 °C and the total reaction volume was adjusted to 240 μl with extraction buffer. 30 μl of the reaction mixture was taken at the indicated time points and 5 μl of 6× SDS loading buffer was added to stop the reaction. For proteasome inhibitor treatments, 30 μM MG132 was added to protein extracts 30 min prior to the start of the assay. ABI5 protein levels were determined by immunoblots using His antibodies (Sigma) at 1:5,000 dilution followed by horseradish peroxidase-conjugated anti-mouse IgG (Sigma) at 1:5,000 dilution.

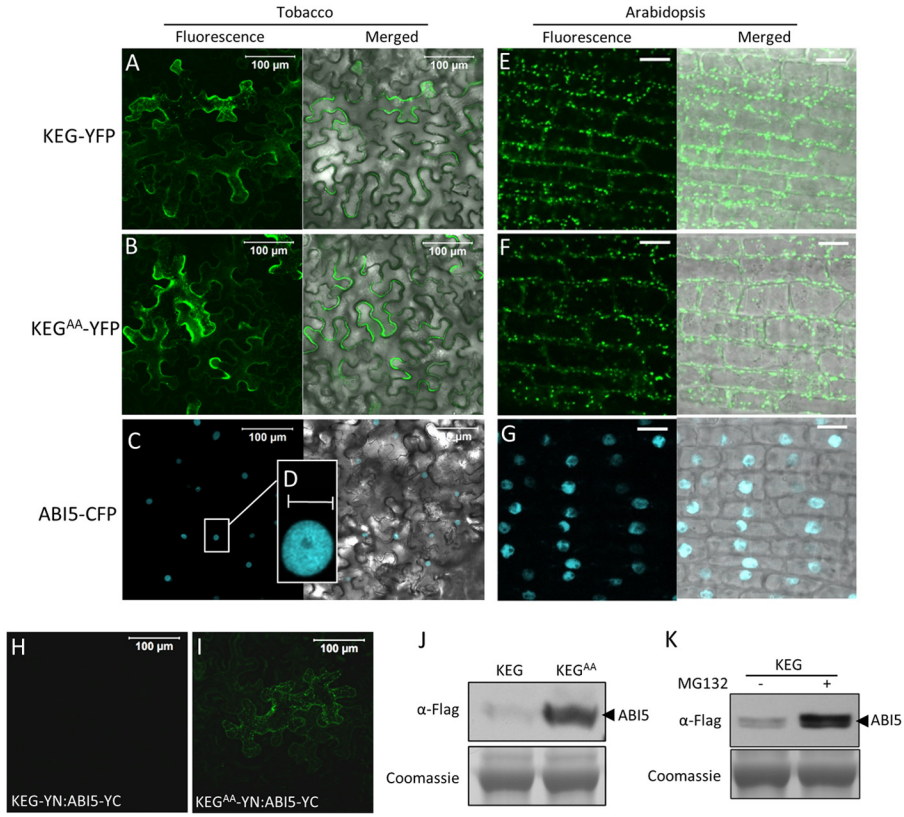

FIGURE 1. **KEG interacts with ABI5 in the cytoplasm.** *A–D*, localization of KEG-YFP (*A*), KEG^{AA}-YFP (*B*), and ABI5-CFP (*C* and *D*) in transiently transformed tobacco leaf epidermal cells. *Right panels* show fluorescence images from a combined series of *Z*-stack. *Left panels* show transmitted light images merged with fluorescence images from a single optical section. *Bars* = 100 μm. *D* displays an enlargement of the section delimited by a *white square* in *C*. *Bar* = 10 μm. *E–G*, localization of KEG-YFP (*E*), KEG^{AA}-YFP (*F*), and ABI5-CFP (*G*) in root cells of transgenic *Arabidopsis* seedlings. *Right panels* show fluorescence images from a single optical section. *Left panels* show transmitted light images merged with fluorescence images from a single optical section. *Bars* = 10 μm. *H* and *I*, BiFC analysis in tobacco epidermal cells. KEG-YN (*H*) or KEG^{AA}-YN (*I*) was coexpressed with ABI5-YC. *Bars* = 100 μm. *J*, levels of ABI5-YC following coexpression with KEG-YN or KEG^{AA}-YN. Analysis was done using protein extracts derived from the same samples assayed for BiFC shown in *H* and *I*. *K*, levels of ABI5-YC in tobacco epidermal cells coexpressing KEG-YN in the absence (−) and presence (+) of MG132. Note: ABI5-YC also contains a FLAG tag. Coomassie staining was used to confirm equal loading.

Abscisic Acid Root Sensitivity Assay—Surface sterilized Col-0 and transgenic seedlings were germinated and grown vertically on solid MS medium for 3 days as described above. Seedlings were then transferred to solid MS medium with or without 2 μM ABA (Sigma) and grown vertically for another 5 days. Root growth after transfer was measured.

RESULTS

KEG Interacts Directly with ABI5 in the Cytoplasm/TGN/EE—KEG has been shown to function as a negative regulator of ABA signaling by modulating the abundance of ABA-responsive transcription factor ABI5 (11, 12). Gu and Innes (13) recently showed that KEG is predominantly localized to the TGN/EE (13). This is in contrast to ABI5, which has been reported to be constitutively localized in the nucleus (14). The results from these subcellular localization studies raise the question of how KEG is able to regulate ABI5 abundance. Does KEG directly interact with ABI5 in plant cells? To address this question we first determined the subcellular localization of KEG and ABI5 in our experimental systems (Fig. 1, *A–G*). Full-length KEG and KEG containing a nonfunctional RING E3 ligase domain (KEG RING mutant; KEG^{AA}) were expressed as C-terminal fusions with YFP under control of the cauliflower mosaic virus 35S promoter in transiently transformed tobacco leaf epidermal cells. Both KEG-YFP and KEG^{AA}-YFP were observed in the cytoplasm as well as small punctate structures reminiscent of the previously observed localization (Fig. 1, *A* and *B*) (13). ABI5 was expressed as a CFP C-terminal fusion (ABI5-CFP) driven by the 35S promoter in transiently transformed tobacco leaf epidermal cells (Fig. 1, *C* and *D*). Unsurprisingly, in our experimental system, ABI5 was observed only in the nucleus (Fig. 1, *C* and *D*). We also generated *Arabidopsis* transgenic plants expressing *ABI5-CFP*, *KEG-YFP*, and *KEG^{AA}-YFP* under the control of the 35S promoter. Localization for KEG-YFP, KEG^{AA}-YFP, and ABI5-CFP in *Arabidopsis* root cells was similar to that observed in transiently transformed tobacco cells (Fig. 1, *E–G*).

To determine whether KEG interacts directly with ABI5, BiFC assays were performed using *Agrobacterium*-mediated transient expression in tobacco leaf epidermal cells. Following co-expression of KEG^{AA} fused with the amino (N)-terminal eYFP fragment (KEG^{AA}-YN) with ABI5 fused with the carboxyl (C)-terminal eYFP fragment (ABI5-YC), BiFC fluorescence signals were observed in the cytoplasm of tobacco epidermal cells indicating that the eYFP fluorophore was reconstituted due to interaction between KEG^{AA} and ABI5 proteins (Fig. 1*I*). However, co-expression of KEG fused to the N-terminal eYFP frag-

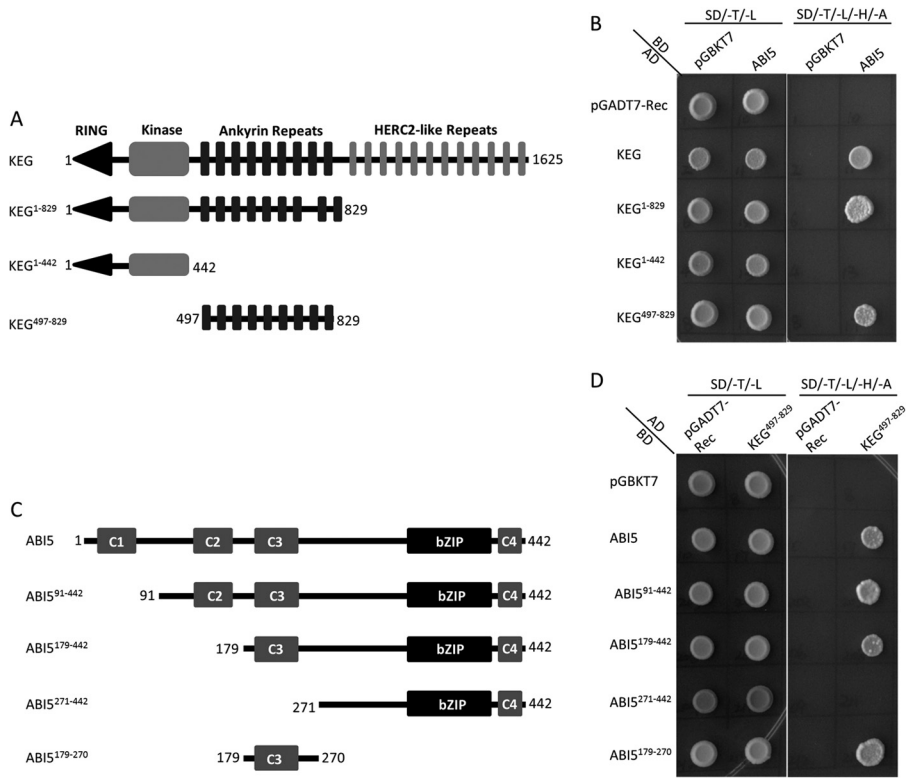

FIGURE 2. **ABI5 conserved C3 domain facilitates interactions with KEG ankyrin repeats.** *A* and *C,* schematic representations of the KEG (*A*) and ABI5 (*C*) used in the yeast two-hybrid assays. *Numbers* indicate amino acids. *B* and *D,* yeast two-hybrid experiments showing interactions between ABI5 and KEG. Full-length *ABI5* cDNA was fused with the GAL4-binding domain (*BD*) and *KEG* constructs (as illustrated in *A*) were fused with the Gal4 activation domain (*AD*) (*B*). Alternatively, *ABI5* cDNA constructs (as illustrated in *C*) were fused to the GAL4-BD and *KEG* cDNA (ankyrin repeats, $KEG^{497-829}$) was fused to the GAL4-AD (*D*). Interaction between ABI5 and KEG was analyzed by growth on selection medium without Trp, Leu, His, and Ade (*SD/-T/-L/-H/-A*). The pGADT7 and pGBKT7-Rec empty vectors were used as negative controls.

ment (KEG-YN) with ABI5-YC did not produce an observable fluorescence signal (Fig. 1*H*). The lack of BiFC signal could be due to the fact that upon interaction, KEG ubiquitinates ABI5 targeting the transcription factor for degradation. To confirm this hypothesis, proteins were extracted from the same leaf sample used for BiFC analysis (Fig. 1, *H* and *I*) and used to determine ABI5 protein levels via immunoblot analysis. As shown in Fig. 1*J*, the ABI5-YC protein was barely detected when co-expressed with KEG-YN. In contrast, ABI5-YC accumulated when co-expressed with KEG^{AA}-YN. To determine whether the low levels of ABI5 observed following co-expression with KEG is due to proteasomal-dependent turnover, tobacco leaves co-expressing ABI5-YC and KEG-YN were incubated with MG132, a specific inhibitor of the 26 S proteasome. As shown in Fig. 1*K*, ABI5 accumulated to greater levels in MG132-treated samples (Fig. 1*K*).

Interactions between KEG and ABI5 are facilitated by the ankyrin repeats of KEG (11, 24), however, the region of ABI5 required for this interaction is not known. Yeast two-hybrid assays were performed to identify the region of ABI5 that mediates interaction with the RING-type E3 ligase. To first demonstrate interactions between KEG and ABI5 in yeast, full-length KEG and a series of KEG truncations ($KEG^{1-442,}$ KEG^{1-829}, and $KEG^{497-829}$) fused with the GAL4 transcriptional activation domain (AD; prey) were co-expressed with full-length ABI5 fused with the GAL4 DNA-binding domain (BD; bait) (Fig. 2*A*). As shown in Fig. 2*B*, interaction is observed between ABI5 and KEG, KEG^{1-829}, or $KEG^{497-829}$. No interaction was observed with KEG^{1-442}, which lacks the ankyrin repeats. ABI5 contains a conserved bZIP DNA-binding domain and four highly conserved regions, C1–C4 (25, 26) (Fig. 2*C*). To determine the region of ABI5 that mediates interaction with KEG, fusions between the GAL4-BD and various regions of ABI5 were tested for interaction with KEG ankyrin repeats ($KEG^{497-829}$) GAL4-AD fusion in yeast (Fig. 2, *C* and *D*). As shown in Fig. 2*D*, a short region of ABI5 that contains the conserved C3 region ($ABI5^{179-270}$) was able to interact with $KEG^{497-829}$. Deletion of the conserved C3 region ($ABI5^{271-442}$) prohibited ABI5 interaction with $KEG^{497-829}$ (Fig. 2*D*).

The Carboxyl-terminal Region of ABI5 Is Required for Protein Turnover—The results described above suggest that KEG modulates ABI5 abundance by interacting with the conserved C3 domain of ABI5 in cytoplasm. To further understand the mechanism underlying KEG regulation of ABI5 turnover, we aimed to determine the region of ABI5 that regulates stability. ABI5-YC ($ABI5^{1-270}$-YC and $ABI5^{1-343}$-YC) lacking the C-terminal region produced a BiFC fluorescence signal when coexpressed with both KEG-YN (Fig. 3, *A*, *B*, and *F*) and KEG^{AA}-YN (Fig. 3, *C* and *G*). This is in contrast to full-length ABI5-YC, which produced a BiFC fluorescence signal only when co-expressed with KEG^{AA}-YN (Fig. 1, *H* and *I*). ABI5-YC lacking the KEG-interacting C3 region ($ABI5^{271-442}$-YC) did not produce a BiFC fluorescence signal when co-expressed with KEG-YN or KEG^{AA}-YN (Fig. 3, *A*, *D,* and *E*). Loss of the C-terminal region

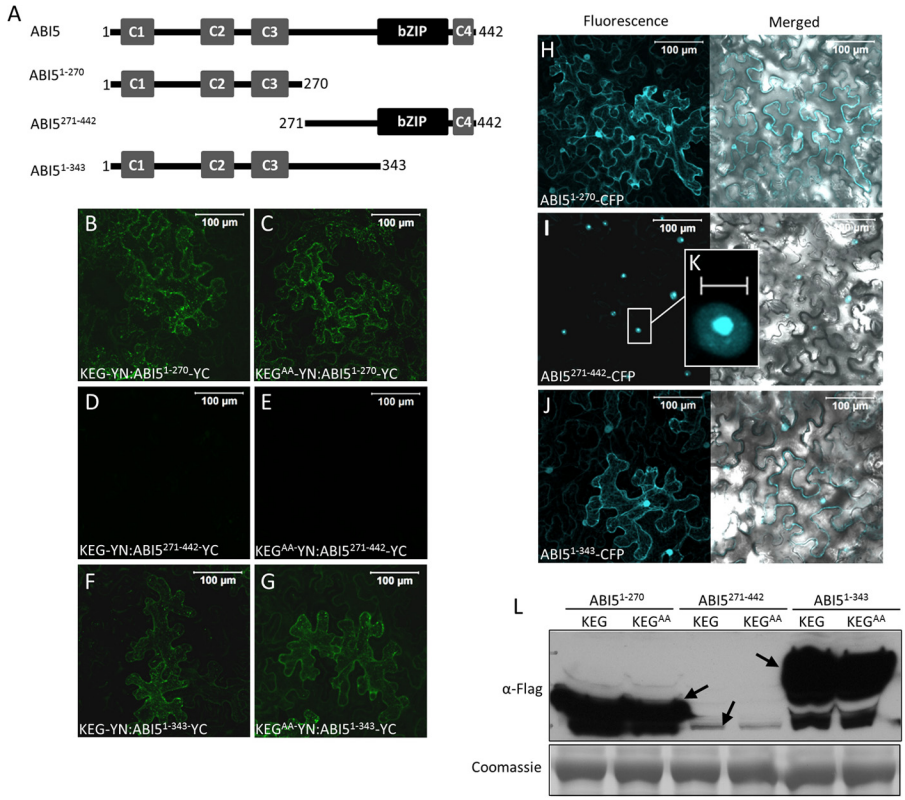

FIGURE 3. **C-terminal region of ABI5 regulates protein stability.** *A,* schematic representation of ABI5 and ABI5 deletion mutants. *Numbers* indicate amino acids. *B–G*, BiFC analysis in tobacco epidermal cells. KEG-YN or KEG^{AA}-YN was coexpressed with ABI5$^{1-270}$-YC (*B* and *C*), ABI5$^{271-442}$-YC (*D* and *E*), or ABI5$^{1-343}$-YC (*F* and *G*). *Bars* = 100 μm. *H–K*, subcellular localizations of ABI5$^{1-270}$-CFP (*H*), ABI5$^{271-442}$-CFP (*I*), and ABI5$^{1-343}$-CFP (*J*) in transiently transformed tobacco epidermal cells. *Left panels* show fluorescent images from a combined series of *Z*-stack. *Right panels* show transmitted light images overlaid with fluorescence images from a single optical section. *Bars* = 100 μm. *K* displays an enlargement of the section delimited by a *white square* in *I*. *Bar* = 10 μm. *L*, levels of ABI5$^{1-270}$-YC, ABI5$^{271-442}$-YC, and ABI5$^{1-343}$-YC were determined following coexpression with KEG-YN or KEG^{AA}-YN. Western blot analysis was done using protein extracts derived from the same tobacco leaf samples assayed for BiFC fluorescence shown in *B–G*. Note: ABI5-YC also contains a FLAG tag. *Arrows* indicate ABI5. Coomassie staining was used to confirm equal loading.

allows for interaction with the functional KEG E3 ligase, which suggests stabilization of ABI5.

If deletion of the C-terminal region of ABI5 stabilizes the transcription factor then the deletion mutants should be observed in the cytoplasm. Localization studies show that ABI5-CFP lacking the C-terminal region was able to accumulate in the cytoplasm. Both ABI5$^{1-270}$-CFP and ABI5$^{1-343}$-CFP were observed in the cytoplasm and nucleus of transiently transformed tobacco epidermal cells (Fig. 3, *H* and *J*). Although the C-terminal region of ABI5 (ABI5$^{271-442}$-CFP) remained exclusively nuclear localized (Fig. 3*I*). In contrast to ABI5-CFP, which is predominantly found in the nucleoplasm (Fig. 1*D*), ABI5$^{271-442}$-CFP was observed mainly in the nucleolus (Fig. 3, *I* and *K*). These results suggests that although KEG is capable of interacting with both ABI5$^{1-270}$ and ABI5$^{1-343}$, the E3 ligase may not be able to target ABI5 lacking the C-terminal region for degradation. Therefore, the ABI5 fusion proteins are observed in the cytoplasm.

To confirm that elimination of the C-terminal region increased protein stability, the levels of ABI5 deletion mutants following co-expression with KEG and KEG^{AA} were determined. The same leaf sample used for BiFC analysis (Fig. 3, *B–G*) was collected, total protein was extracted, and ABI5 protein levels were determined via immunoblot analysis. Unlike ABI5-YC (Fig. 1*J*), equally high levels of ABI5$^{1-270}$-YC and ABI5$^{1-343}$-YC accumulated when co-expressed with both KEG-YN (Fig. 3*L*, *fifth* and *first lanes*) and KEG^{AA}-YN (Fig. 3*L*, *second* and *sixth lanes*). These results are consistent with localization and BiFC studies, which suggested that KEG is unable to target ABI5 lacking the C-terminal region for degradation. Unexpectedly, low levels of the ABI5$^{271-442}$-YC, which lacks the KEG-interacting C3 region, were observed following co-expression with both KEG-YN and KEG^{AA}-YC (Fig. 3*L*, *third* and *fourth lanes*). Reasons for this are outlined under "Discussion."

Cell-free degradation assays were used to compare the stability of ABI5 and ABI5$^{1-343}$, which lack the C-terminal region. Recombinant FLAG-His-ABI5 or FLAG-His-ABI5$^{1-343}$ were incubated with protein extracts prepared from wild type or *keg-1* seedlings in the presence or absence of MG132. Using wild type protein extracts, the levels of FLAG-His-ABI5 gradually decreased over time (Fig. 4*A*). The decrease in FLAG-His-ABI5 levels was considerably slower in *keg-1* protein extracts demonstrating the involvement of KEG activity in the turnover of ABI5 in the experimental system (Fig. 4*A*). The turnover of ABI5 was also greatly reduced in the presence of proteasome inhibitor, MG132 (Fig. 4*B*). In contrast to FLAG-His-ABI5, decreases in FLAG-His-ABI5$^{1-343}$ levels were significantly slowed in the absence of MG132 (Fig. 4*B*), further demonstrating the involvement of the ABI5 C-terminal region in regulating protein stability.

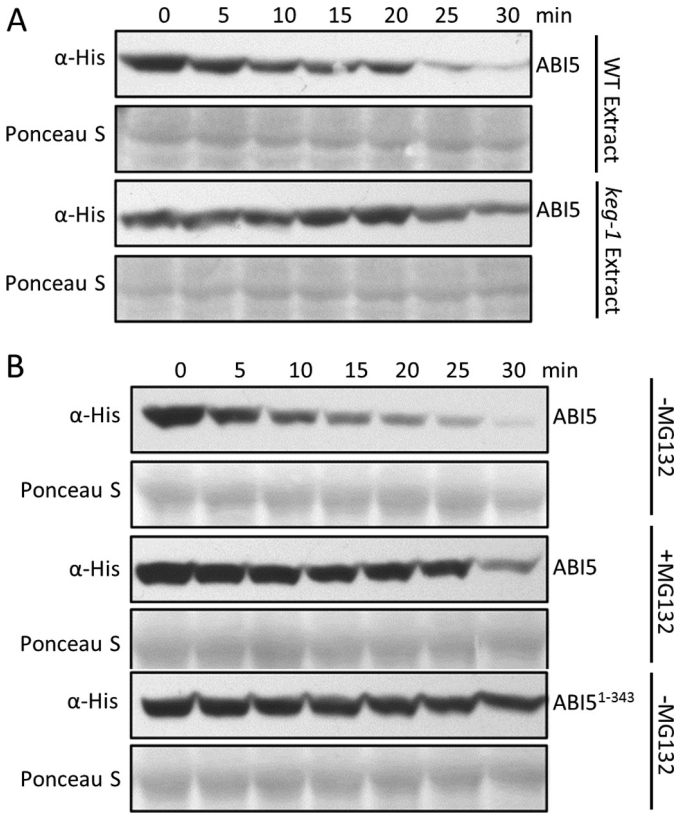

FIGURE 4. **Turnover of ABI5 in cell-free degradation assays requires proteasome activity, KEG, and ABI5 C-terminal region.** *A,* comparison of recombinant FLAG-His-ABI5 turnover in wild type (WT) *Arabidopsis* or *keg-1* plant extracts. *B,* turnover of recombinant FLAG-His-ABI5 and FLAG-His-ABI5$^{1-343}$ in WT protein extracts in the presence (+) or absence (−) of 30 μM MG132. ABI5 protein levels were determined by Western blotting using His antibodies. Ponceau S staining was used to confirm equal loading.

The Carboxyl-terminal Region Modulates Localization as Well as Stability of ABI5—The fact that ABI5 interacts with KEG and stabilized ABI5 is observed in the cytoplasm suggests that the transcription factor is shuttled between the nucleus and the cytoplasm. Amino acid sequence analysis of ABI5 identified a potential N-terminal nuclear export signal (NES; ^{37}LGRQSSIYSLTL^{48}) and three potential nuclear localization signals (NLSs) within the C-terminal region, referred to as NLS1-NLS3 (Fig. 5). To confirm the presence of functional NLSs a series of CFP-FLAG-tagged ABI5 deletion mutants were generated, and subcellular localization was observed in transiently transformed tobacco epidermal cells (Fig. 6, *A–F*). Deletion of the NLS1/2 region (ABI5$^{\Delta 344-376}$-CFP) resulted in a mixed localization pattern with some cells showing both nuclear and cytoplasmic localization and the remaining cells showing only a nuclear localization (Fig. 6*B*). Within the cytoplasm ABI5$^{\Delta 344-376}$-CFP was observed in small punctuate structures similar to that observed for KEG-YFP (Fig. 1, *A* and *B*). The fact that ABI5$^{\Delta 344-376}$-CFP localized predominantly to the nucleus in many cells suggests that NLS1 and NLS2 may not be necessary for nuclear localization. The observed cytoplasmic localization for ABI5$^{\Delta 344-376}$-CFP in some cells may instead be due to stabilization of the fusion protein. To determine whether this was the case, ABI5$^{\Delta 344-376}$-YC was co-expressed with KEG-YN or KEG^{AA}-YN in transiently transformed tobacco cells. ABI5$^{\Delta 344-376}$-YC interacted with both KEG-YN and KEG^{AA}-YN, as determined by the presence of BiFC fluorescence signals (Fig. 6, *G* and *L*), indicating that KEG may not target ABI5 lacking NLS1/2 (amino acids 344–376) for degradation. Deletion of NLS3 (ABI5$^{\Delta 406-409}$) or NLS3 plus surrounding amino acids (ABI5$^{\Delta 377-409}$ and ABI5$^{\Delta 406-442}$) did not alter the localization of ABI5-CFP, all fusion proteins were observed exclusively in the nucleus of tobacco epidermal cells (Fig. 6, *C*, *D*, and *F*). BiFC assays showed that ABI5$^{\Delta 377-409}$-YC, ABI5$^{\Delta 406-409}$-YC, and ABI5$^{\Delta 406-442}$-YC produced a fluorescence signal when co-expressed with KEG^{AA}-YN (Fig. 6, *M*, *N*, and *P*) but not with KEG-YN (Fig. 6, *H*, *I*, and *K*). These results suggest that, unlike loss of NLS1/2, deletion of NLS3 or NLS3 plus surrounding regions does not influence the stability of ABI5. Because deletion of NLS1/2 or NLS3 alone did not result in predominantly cytoplasmic localization of ABI5, the NLS1/2 and NLS3 deletions were combined (ABI5$^{\Delta 344-376,\Delta 406-409}$). ABI5$^{\Delta 344-376,\Delta 406-409}$-CFP was observed mainly in the cytoplasm (Fig. 6*E*). BiFC analysis demonstrate interaction between ABI5$^{\Delta 344-376,\Delta 406-409}$-YC and both KEG-YN and KEG^{AA}-YN (Fig. 6, *J* and *O*). Thus, loss of NLS1/2 (amino acids 344–376) in conjunction with deletion of NLS3 (amino acids 406–409) resulted in stabilization and accumulation of ABI5 in the cytoplasm.

To compare the stability of the different ABI5 deletion mutants in the presence of KEG, protein extracts were prepared from the same leaf samples used for BiFC analysis (Fig. 6, *G–K*) and ABI5 levels were determined via immunoblot analysis (Fig. 6*Q*). Consistent with the localization and BiFC results, ABI5 lacking the NLS1/2 region (ABI5$^{\Delta 344-376}$-YC) accumulated to significantly higher levels than ABI5 with only the NLS3 region deleted (ABI5$^{\Delta 337-409}$ and ABI5$^{\Delta 406-409}$-YC) (Fig. 6*Q*, compare *first lane* to *second* and *third lanes*). In addition, deletion of the NLS1/2 region in conjunction with NLS3 (ABI5$^{\Delta 344-376,\Delta 406-409}$-YC) resulted in even greater accumulation of ABI5 (ABI5$^{\Delta 344-376}$-YC) (Fig. 6*Q, fourth lane*). These results provide further evidence for the stabilizing effects of deleting NLS1/2 (amino acids 344–376) on the ABI5 protein. Surprisingly, nuclear-localized ABI5$^{\Delta 406-442}$-YC accumulated to much higher levels compared with other nuclear-localized ABI5 mutants (ABI5$^{\Delta 337-409}$-YC and ABI5$^{\Delta 406-409}$-YC) (Fig. 6*Q*, compare *fifth lane* to *second* and *third lanes*).

Lysine 344 Is Involved in ABI5 Turnover—The above results suggest that residues within the 344–376 range of amino acids are involved in turnover of ABI5. Within this region there are four lysine residues (Lys^{344}, Lys^{353}, Lys^{364}, and Lys^{376}), which may serve as attachment sites of ubiquitin (Fig. 5). To determine whether one or more of these lysines are involved in degradation of ABI5, pairs of lysine residues were first changed to alanine and the ABI5 mutants were transiently expressed in tobacco cells as CFP fusion proteins (Fig. 7, *A–C*). Accumulation of the mutant ABI5 in the cytoplasm would indicate increased stability of the fusion protein. Replacing Lys^{344} and Lys^{353} (ABI5$^{K344/353A}$-CFP) or Lys^{364} and Lys^{376} (ABI5$^{K364/376A}$-CFP) with alanine did not result in any visible accumulation of ABI5-CFP in the cytoplasm (Fig. 7, *B* and *C*). The lack of cytoplasmic localization may be due to the presence of NLS3, which would direct

Basic Region — Leucine Zipper

```
AT2G36270 ABI5     RGRKRVVDGPVEKVVERRQRRMIKNRESAARSRARKQAYTVELEAELNQLKEENAQLKHALAEL
AT1G03970 GBF4     GKRGRVMMEAMDKAAAQRQKRMIKNRESAARSRERKQAYQVELETLAAKLEEENEQLLKEIEES
AT5G42910 bZIP15   GGKINSEITAEKQFVDKKLRRKIKNRESAARSRARKQAQTMEVEVELENLKKDYEELLKQHVEL
AT3G19290 ABF4     LNRGRRSNTGLEKVIERRQRRMIKNRESAARSRARKQAYTLELEAEIEKLKKTNQELQKKQAEM
AT1G45249 ABF2     GGVRGRKSGTVEKVVERRQRRMIKNRESAARSRARKQAYTVELEAEVAKLKEENDELQRKQARI
AT1G49720 ABF1     FGRGRRSNTGLEKVVERRQKRMIKNRESAARSRARKQAYTLELEAEIESLKLVNQDLQKKQAEI
AT4G34000 ABF3     FGRVRKTGAVLEKVIERRQKRMIKNRESAARSRARKQAYTMELEAEIAQLKELNEELQKKQVEI
AT4G35900 bZip14   SFGKKRGQDSNEGSGNRRHKRMIKNRESAARSRARKQAYTNELELEVAHLQAENARLKRQQDQL
AT5G44080 bZIP13   GKRARVMVEPLDKAAAQRQRRMIKNRESAARSRERKQAYQVELEALAAKLEEENELLSKEIEDK
AT3G44460 DPBF2    RIKKRIIDGPPEILMERRQRRMIKNRESAARSRARRQAYTVELELELNNLTEENTKLKEIVEEN
AT2G41070 EEL      PGRKRVAGEIVEKTVERRQKRMIKNRESAARSRARKQAYTHELEIKVSRLEEENEKLRRLKEVE
AT2G17770 BZIP27   CLGKKRGQDSDDTRGDRRYKRMIKNRESAARSRARKQAYTNELELEIAHLQTENARLKIQQEQL
AT3G56850 AREB3    GRKRVASGEVVEKTVERRQKRMIKNRESAARSRARKQAYTHELEIKVSRLEEENERLRKQKEVE
```

C4

```
AT2G36270 ABI5     ERKRKQQYFESLKSRAQPKLPKSNGRLRTLMRNPSCPL
AT1G03970 GBF4     TKERYK---KLMEVLIPVDEKPRP-PSRPLSRSHSLEW
AT5G42910 bZIP15   RKRQMEPG--MISLHER--------PERKLRRTKSDIK
AT3G19290 ABF4     VEMQKNE--QLKETSKRPWGS----KRQCLRRTLTGPW
AT1G45249 ABF2     MEMQKN-----QETEMRNLLQGG--PKKKLRRTESGPW
AT1G49720 ABF1     MKTHNS---ELKEFSKQPPLLA---KRQCLRRTLTGPW
AT4G34000 ABF3     MEKQKN---QLLEPLRQPWGMGC--KRQCLRRTLTGPW
AT4G35900 bZip14   K---------MAAAIQQP-------KKNTLQRSSTAPF
AT5G44080 bZIP13   RKERYQ---KLMEFVIPVVEKPKQQPPRFLRRIRSLEW
AT3G44460 DPBF2    EKKRRQ---EIISRSKQVTKEKSGDKLRKIRRMASAGW
AT2G41070 EEL      K---------ILPSEPPPD------PKWKLRRTNSASL
AT2G17770 BZIP27   K---------IAEATQNQ-------VKKTLQRSSTAPF
AT3G56850 AREB3    K---------ILPSVPPPD------PKRQLRRTSSAPF
```

FIGURE 5. **Schematic representation of ABI5 and amino acid sequence alignment of the C-terminal region of *A. thaliana* ABI5-related bZIP transcription factors.** *Arrows* delineated the region of ABI5 shown in the alignment. The basic region and leucine zipper of the bZIP DNA-binding domain and the conserved C4 region are *outlined*. The positions of the predicted nuclear localization signals, NLS1 (*bold and underlined*), NLS2 (*bold and italics*), and NLS3 (*bold*), of ABI5 are highlighted. ABI5 lysine residues (Ly^{344}, Lys^{353}, Lys^{364}, and Lys^{376}) mutated in this study are marked by *asterisks* (*).

the stabilized ABI5 to the nucleus. To address this issue, NLS3 (amino acids 406–409) deletion was combined with the lysine mutations (ABI5$^{K344/353A,\Delta406-409}$-CFP and ABI5$^{K364/376A,\Delta406-409}$-CFP). As shown in Fig. 7*D*, ABI5$^{K344/353A,\Delta406-409}$-CFP was observed in the cytoplasm as well as the nucleus. In contrast, ABI5$^{K364/376A,\Delta406-409}$-CFP was still only observed in the nucleus (Fig. 7*E*). These results indicate that Lys^{344} or Lys^{353} is utilized for targeting cytoplasmic ABI5 for degradation.

To distinguish between the requirement for Lys^{344} and/or Lys^{354}, single lysine to alanine substitutions were combined with deletion of NLS3 (ABI5$^{K344A/\Delta406-409}$-CFP and ABI5$^{K353A,\Delta406-409}$-CFP) (Fig. 7, *A*, *F,* and *G*). Replacing Lys^{344} with alanine was sufficient for significant accumulation of ABI5$^{K344A,\Delta406-409}$-CFP in the cytoplasm (Fig. 7*F*), whereas loss of K353 did not affect localization of ABI5$^{K353A,\Delta406-409}$-CFP (Fig. 7*G*). Consistent with the localization studies, immunoblot analysis showed that ABI5$^{K344A,\Delta406-409}$-CFP (Fig. 7*H*, *lane 1*) accumulated to much higher levels compared with ABI5$^{K353A,\Delta406-409}$-CFP in the tobacco cells (Fig. 7*H*, *lane 2*). Using BiFC analysis, ABI5$^{K344A,\Delta406-409}$-YC was found to interact with both KEG-YN and KEG^{AA}-YN (Fig. 7, *I* and *J*). In contrast, ABI5$^{K353A,\Delta406-409}$-YC was found to produce BiFC fluorescence signals with KEG^{AA}-YN and not with KEG-YN (Fig. 7, *K* and *L*). These results suggest that Lys^{344} is involved in turnover of ABI5. The levels of ABI5$^{K344A,\Delta406-409}$-YC and ABI5$^{K353A,\Delta406-409}$-YC following co-expression with KEG-YN were also determined. The same leaf samples used for BiFC analysis (Fig. 7, *I* and *K*) were collected, and ABI5 protein levels were determined via immunoblot analysis. Compared with ABI5$^{K353A,\Delta406-409}$-YC, significantly higher levels of ABI5$^{K344A,\Delta406-409}$-YC accumulated when co-expressed with KEG-YN (Fig. 7*M*). These results are consistent with the BiFC analysis, which suggested that KEG does not promote the turnover of ABI5 lacking Lys^{344}.

To further assess the role of lysine 344 in the turnover of ABI5, transgenic *Arabidopsis* plants expressing CFP-tagged wild type and mutant versions of ABI5 were generated and used for localization studies. Two independently generated transgenic lines were obtained for each transgene. Similar to ABI5-CFP, ABI5^{K344A}-CFP and ABI5$^{\Delta406-409}$-CFP are observed only within the nucleus of *Arabidopsis* root cells (Fig. 8, *A–C*). However, ABI5$^{K344A,\Delta406-409}$-CFP was observed within the nucleus and cytoplasm (Fig. 8*D*). Therefore, similar to results obtained using tobacco cells (Fig. 7*F*), loss of lysine 344 in conjunction with deletion of NLS3 (amino acids 406–409) resulted in stabilization of ABI5 and accumulation of the transcription factor in the cytoplasm.

To ensure that the cytoplasmic localization of ABI5 is due to stabilization and not to accumulation of a nonfunctional protein, the ability of transgenic seedlings to respond to ABA was assessed. There were no observable differences between wild type and transgenic seedlings grown in the absence of ABA (Fig. 8*E*). Similar to overexpression of ABI5-CFP, transgenic seedlings overexpressing ABI5^{K344A}-CFP, ABI5$^{\Delta406-409}$-CFP, or ABI5$^{K344A,\Delta406-409}$-CFP were sensitive to the inhibitory effects of ABA on primary root elongation (Fig. 8, *E* and *F*). This demonstrates that the mutant versions of ABI5 are functional and capable of facilitating plant response to ABA.

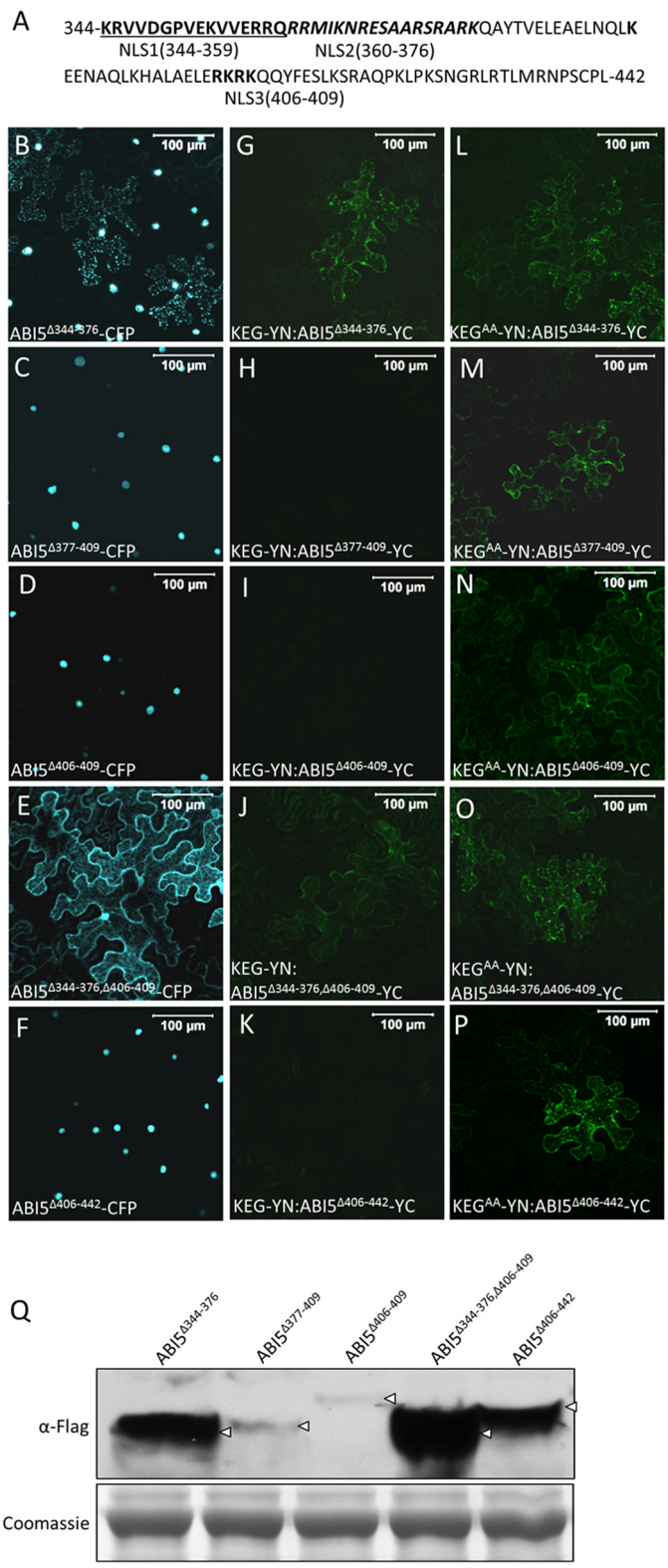

FIGURE 6. **Delineating the region of ABI5 required for KEG-mediated ubiquitination.** *A,* amino acid sequence of ABI5 C-terminal region showing the positions of the deleted regions, NLS1 (*bold and underlined*), NLS2 (*bold and italics*), and NLS3 (*bold*). *B–F*, subcellular localization of the CFP-ABI5 deletion mutants in transiently transformed tobacco leaf epidermal cells. Fluorescence images are a combined series of *Z*-stack. *G–P*, BiFC assay in tobacco leaf epidermal cells. KEG-YN or KEG^{AA}-YN was coexpressed with the indicated ABI5-YC deletion mutant. *Numbers* indicate the deleted (Δ) amino acids for each ABI5 mutant. *Bars* = 100 μm. *Q,* levels of each ABI5-YC deletion mutant following coexpression with KEG-YN. Analysis was done using protein extracts derived from the same tobacco leaf samples assayed for BiFC fluorescence shown in *G–K*. Note: ABI5-YC also contains a FLAG tag. *Arrows* indicate ABI5. Coomassie staining was used to confirm equal loading.

DISCUSSION

Our findings demonstrate that KEG directly interacts with the transcription factor ABI5 and this interaction is critically involved in the regulation of ABI5 abundance. This conclusion is based on a number of supporting observations. First, despite the apparent differences in subcellular localization KEG interacts directly with ABI5 in the cytoplasm/TGN/EE. The interaction occurs via the conserved C3 region of ABI5 and KEG ankyrin repeats. Second, using BiFC analysis, we were only able to detect interactions between KEG and ABI5 following inactivation of the KEG RING E3 ligase domain, suggesting turnover of ABI5 by the functional KEG protein. In addition, ABI5 was found to accumulate in tobacco cells co-expressing the KEG RING mutant but not in cells co-expressing wild type KEG. Furthermore, treatment of tobacco cells co-expressing KEG and ABI5 with proteasome inhibitors resulted in accumulation of ABI5. These results support the notion that KEG binds to and ubiquitinates ABI5, which is then degraded by the 26 S proteasome. Finally, using deletion mutants, we show that the C-terminal region of ABI5 regulates stability. Specifically, we demonstrate that lysine 344 is involved in turnover of ABI5 in the cytoplasm. Loss of the C-terminal region of ABI5 or elimination of lysine 344 stabilizes ABI5 resulting in accumulation of the transcription factor in the cytoplasm and also facilitates interactions with wild type KEG. Overall, this study provides strong evidence for the functional relationship between ABI5 and KEG.

ABI5 and ABI5-related bZIP transcription factors (AREBs (ABA responsive element-binding proteins), ABFs (ABRE binding Factors), and/or DPBFs (Dc3 promoter binding factors)), all possess similar domain architecture, consisting of a bZIP DNA-binding domain and four highly conserved regions, C1–C4 (25–27). The interaction between KEG and ABI5 occurs via the conserved C3 region of ABI5. Therefore, it is possible that KEG may also interact with and regulate other family members. However, lysine 344, which is required for KEG regulation of ABI5 abundance, is less conserved among other family members (Fig. 5). For most ABI5-related proteins, a lysine residue can be found within the surrounding amino acids. However, a similarly positioned lysine residue is not the only criteria that may determine regulation by KEG. In addition to the position of the ubiquitin acceptor site, the amino acid sequence or local structure surrounding the site also serves as a determinant for degron function (4). These factors may work together to decide the substrate specificity for KEG among the ABI5-related transcription factors. Nevertheless, this work opens the way to study the regulation of the other ABI5-related bZIP transcription factors.

ABI5 is predicted to be a nucleocytoplasmic protein. Movement across the nuclear envelope requires the presence of nuclear import and export signals, which are recognized by receptor proteins that mediate nucleocytoplasmic transport (28). The position of these signals within the shuttled protein is also of importance because they must be accessible to the

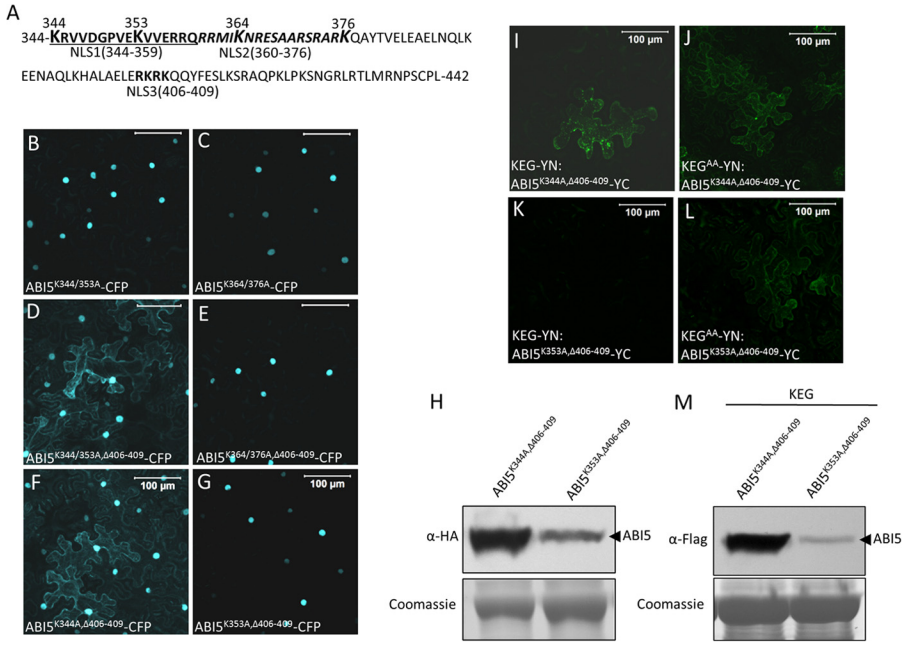

FIGURE 7. **Lysine 344 of ABI5 is involved in protein stability and KEG-dependent turnover.** *A,* amino acid sequence of the ABI5 C-terminal region showing lysine (*K*) residues that were changed to alanine (*A*). *B–G,* subcellular localization of the indicated ABI5-CFP mutants in transiently transformed tobacco epidermal cells. Fluorescent images represent a combined series of *Z*-stack. *H,* protein levels of ABI5$^{K343A/\Delta406-409}$-CFP and ABI5$^{K343A/\Delta406-409}$-CFP. Analysis was done using protein extracts derived from the same tobacco leaf samples assayed for localization shown in *F* and *G*. Note: ABI5-CFP also contains a HA tag. *I–L,* BiFC assays in tobacco epidermal cells. KEG-YN or KEG^{AA}-YN was coexpressed with the indicated ABI5-YC mutant. *Bars* = 100 μm. *M,* levels of ABI5$^{K343A/\Delta406-409}$-YC and ABI5$^{K343A/\Delta406-409}$-YC following co-expression with KEG-YN. Analysis was done using protein extracts derived from the same tobacco leaf samples assayed for BiFC fluorescence shown in *I* and *K*. Note: ABI5-YC also contains a FLAG tag. Coomassie staining was used to confirm equal loading.

nuclear transport machinery (28, 29). ABI5 is predicted to contain two basic NLSs and a leucine-rich NES, which may facilitate nucleocytoplasmic transport. Although the presented results suggest nucleocytoplasmic localization further experiments are required to demonstrate that the predicted NLS and NES sequences are directly involved in the transport of ABI5 across the nuclear envelope. Additional experiments are also required to determine how nuclear import and export of ABI5 may be regulated. The presence of the NLS and NES sequences also suggests that subcellular relocalization may play a role in regulating ABI5 function. Many transcription factors are regulated in this manner including bZIP-type repression of shoot growth (RSG) and common plant regulatory factor 2 (CPRF2), which are retained in the cytoplasm and relocalized to the nucleus in response to external signals such as light or stress (30, 31). However, relocalization may not be the major regulatory step in modulating ABI5 function. Instead, in the absence of ABA, ABI5 seems to be turned over by the ubiquitin proteasome system within the cytoplasm. Evidence provided in this and previous studies demonstrates that KEG interacts with and ubiquitinates ABI5 targeting the protein for proteasomal degradation (11). The KEG-dependent turnover of ABI5 within the cytoplasm may account for the constitutive nuclear localization observed for the transcription factor (14, 15). This notion is supported by the fact that mutations in ABI5 such as deletions within the C-terminal region (*e.g.* amino acids 344–376) or replacing lysine 344 with alanine, which prohibit degradation and allow for interactions with KEG, facilitate accumulation of ABI5 in the cytoplasm. Based on the results, the C-terminal region of ABI5 seems to regulate both nuclear localization as well as stability. This would explain the mainly cytoplasmic localization of ABI5 when the entire C-terminal region is deleted. Also, ABI5 lacking a nuclear localization signal (NLS3) is only observed in the cytoplasm when the deletion is combined with the stabilizing lysine 344 to alanine mutation. In response to ABA or stress, ABI5 levels increase dramatically due in part to a reduction in proteasomal degradation (7, 9). ABA has been shown to promote KEG self-ubiquitination and subsequent degradation by the proteasome, which would allow for accumulation of ABI5 (12). Despite the decrease in ubiquitin-dependent turnover, ABI5 is not observed in the cytoplasm in the presence of the hormone (14). This is most likely due to the predicted nuclear localization signals, which may immediately shuttle the stabilized transcription factor into the nucleus.

Mutant analysis identified two regions within the C-terminal end of ABI5 that modulate protein stability. As discussed above, the first region containing lysine 344 (amino acids 344–376) is involved in KEG-mediated turnover of ABI5 in the cytoplasm. A second region may reside within amino acids 410–442. ABI5 deletion mutants, ABI5$^{\Delta377-409}$, ABI5$^{\Delta406-409}$, and ABI5$^{\Delta406-442}$ are only observed in the nucleus and all are potential targets for KEG E3 ligase activity (Fig. 6). However, when co-expressed with KEG, ABI5 mutants lacking amino acids 410–442 (ABI5$^{\Delta406-442}$) accumulate to much higher levels compared with other deletion mutants (ABI5$^{\Delta377-409}$ and ABI5$^{\Delta406-409}$) that contain these amino acids (Fig. 6*Q*). This suggests the presence of another E3 ligase, possibly nuclear localized, which contributes to the turnover of ABI5. The actions of a nuclear-localized E3 ligase may account for the significantly higher accumulation of ABI5$^{\Delta344-376,\Delta406-409}$, which combines dele-

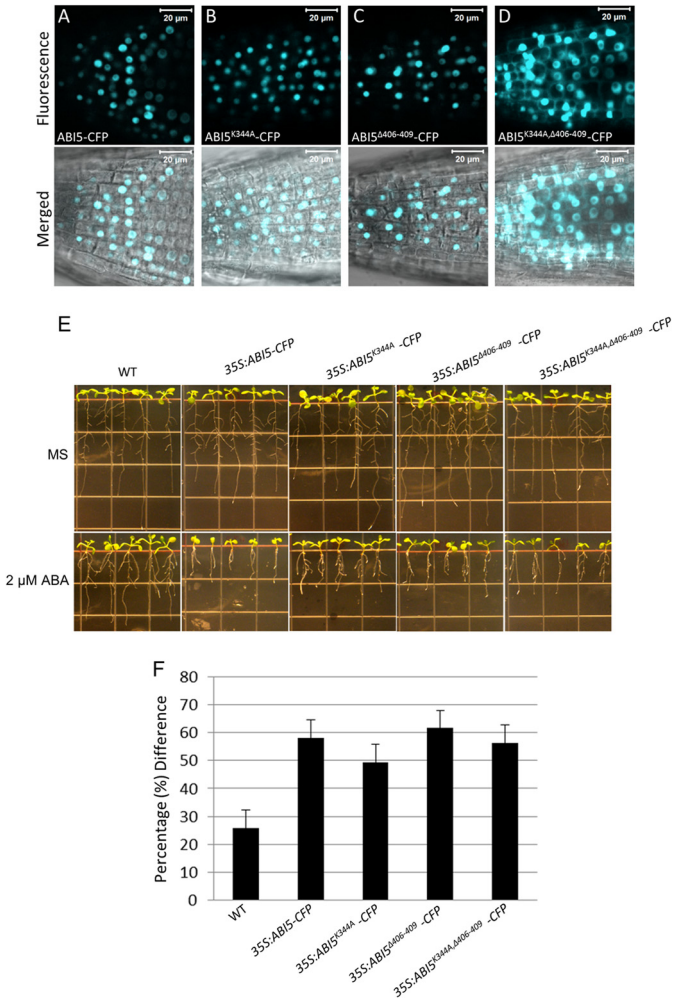

FIGURE 8. **Effects of the lysine 344 mutation on ABI5 localization and function in *Arabidopsis*.** *A–D*, localization of ABI5-CFP, ABI5^{K344A}-CFP, ABI5$^{\Delta 406-409}$-CFP, and ABI5$^{K344A,\Delta 406-409}$-CFP in root cells of transgenic *Arabidopsis* seedlings. *Upper panels* show fluorescence images from a single optical section. *Lower panels* show transmitted light images merged with fluorescence images from a single optical section. *Bars* = 20 μm. *E*, ABA root sensitivity assays. 8-Day-old wild type (WT) and transgenic seedlings expressing CFP-ABI5 or the indicated CFP-ABI5 mutant were grown for 5 days without (*top panels*) or with 2 μM ABA (*bottom panel*). *F*, the graph illustrates the percentage difference in root length between ABA-treated (2 μM) and untreated roots for each genotype. *Error bars* represent mean ± S.E.

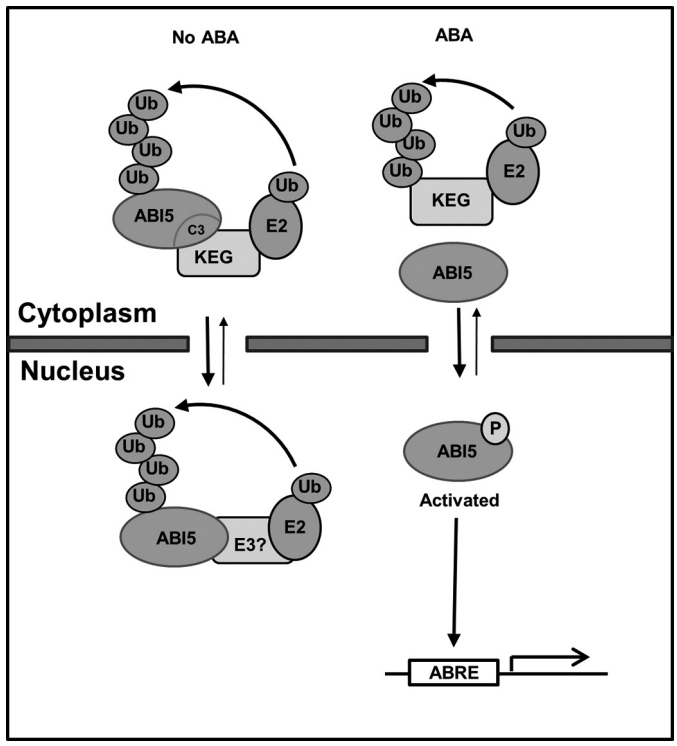

FIGURE 9. **Model for regulating ABI5 protein abundance in the absence and presence of ABA.** In the absence of ABA, KEG interacts with the C3 domain of ABI5, ubiquitinates and targets ABI5 for degradation by the proteasome in the cytoplasm. Another E3 may regulate the abundance of nuclear ABI5 utilizing amino acids 410–442. In response to ABA, ABI5 accumulates due to increase transcription and impediment of KEG E3 activity by ABA-mediated KEG self-ubiquitination and degradation. ABI5 is activated by phosphorylation, which leads to the expression of ABA-responsive genes. When the activity of ABI5 is no longer required or needs to be reduced, the transcription factor is degraded by other E3s such as DWA1/2 containing Cullin-based RING E3 ligase.

tion of amino acids 344–376 and a nuclear localization signal (NSL3), compared with ABI5$^{\Delta 344-376}$ that only lacks amino acids 344–376 (Fig. 6*Q*). Impaired nuclear localization would prohibit degradation by the unknown nuclear localized E3, further reducing the turnover of ABI5. Alternatively, the difference in protein levels may be due to variations in expression, however, this is unlikely as the results shown are consistently observed over independently repeated trials. The presence of another E3 ligase that targets ABI5 for degradation may also account for the increase in ABI5 levels observed following treatment of *keg-1* seedlings with ABA (11). Additionally, the rise in ABI5 levels seen in ABA-treated *keg-1* seedlings can be attributed to an increase in transcript levels.

The abundance of ABI5 is regulated by ABA at both the transcriptional and post-translational levels. ABI5 transcript is abundant in developing and mature/dried seeds (6, 7). Post-germination, the ABI5 transcript is undetectable but increases in the presence of ABA via the action of multiple ABI loci including *ABI5*, *ABI3*, and *ABI4* (6, 7). Similar to *ABI5*, *ABI3* and *ABI4* encode for transcription factors that may directly regulate *ABI5* expression (7, 8). Post-translation regulation of ABI5 abundance requires the function of multiple E3 ligases (10). Each E3 ligase seems to regulate ABI5 abundance under certain circumstances and within specific subcellular compartments. A Cullin-based RING E3 ligase complex, which utilize DWD hypersensitive to ABA 1 (DWA1) and DWA2 as substrate receptors has also been identified as a negative regulator of ABI5 protein abundance (32). Evidence for DWA1/2 involvement in regulating ABI5 abundance comes from the observation that *dwa1* or *dwa2* single or double mutant plants accumulate higher levels of ABI5 than wild type plants following treatment with ABA (32). Although KEG and DWA1/2 regulate ABI5 stability they do so under different circumstances. KEG functions to keep ABI5 low in the absence of ABA, whereas DWA1 and DWA2 ubiquitinate ABI5 in the nucleus to possibly attenuate the ABA response. Evidence supporting these assumptions is as follows. First, KEG is localized in the cytoplasm/TGN/EE, whereas DWA1 and DWA2 heterodimer is found in the nucleus. Second, *keg* seedlings exhibit strong post-germinative growth arrest without the need for ABA treatment. By contrast, *dwa1* and *dwa2* mutants do not show any phenotypic differences compared with the wild type in the absence of

ABA. Third, ABI5 is strikingly up-regulated in *keg* seedlings regardless of the presence or absence of the hormone, whereas ABI5 is not detectable in *dwa1* and *dwa2* and only accumulates after ABA treatment. Thus KEG and DWA1/2 function cooperatively to modulate ABI5 stability to ensure that protein levels remain low in the absence of ABA or stress stimuli and then kept in check so that the plant can recover following removal of the stress stimulus.

Based on this and previous reports, a model is suggested for modulation of ABI5 abundance (Fig. 9). The presence of both potential nuclear localization and export signals suggests that ABI5 protein is continually shuttled between the nucleus and cytoplasm. Post-germination, in the absence of ABA, the ABI5 transcript and protein levels are low. Turnover of the ABI5 protein involves KEG-mediated ubiquitination and subsequent degradation by the proteasome in the cytoplasm. The KEG-interacting ABI5 may be a nuclear-exported transcription factor that accumulated in developing/mature seeds. In seeds/seedlings lacking KEG function, this pool of ABI5 would be stable and arrest growth post-germination. Additionally, another E3 may regulate nuclear ABI5 through amino acid residues 410–442 to further ensure that ABI5 function is fully suppressed. In response to ABA, ABI5 protein accumulates via increased transcription and decrease in proteasomal degradation. The increase in ABI5 abundance is due in part to the impediment of KEG E3 activity by ABA-induced KEG self-ubiquitination and subsequent degradation. Nuclear ABI5 is activated by phosphorylation and modulates the expression of ABA-responsive genes. When the function of ABI5 is no longer required or needs to be reduced, the transcription factor is degraded by nuclear-localized E3s, such as DWA1 and DWA2 containing Cullin-based RING E3 ligases.

Acknowledgments—We thank Dr. Yuhai Cui for kindly providing the pEarleygate201-YN, pEarleygate202-YC, pGBKT7-DEST, and pGADT7-DEST vectors and Dr. Judy Callis for providing keg seeds. We thank Wendy Lyzenga and Daryl McNeilly for reading of the manuscript.

REFERENCES

1. Vierstra, R. D. (2009) The ubiquitin-26S proteasome system at the nexus of plant biology. *Nat. Rev. Mol. Cell Biol.* **10,** 385–397
2. Hammond-Martel, I., Yu, H., and Affar el, B. (2012) Roles of ubiquitin signaling in transcription regulation. *Cell. Signal.* **24,** 410–421
3. Strieter, E. R., and Korasick, D. A. (2012) Unraveling the complexity of ubiquitin signaling. *ACS Chem. Biol.* **7,** 52–63
4. Ravid, T., and Hochstrasser, M. (2008) Diversity of degradation signals in the ubiquitin-proteasome system. *Nat. Rev. Mol. Cell Biol.* **9,** 679–690
5. Radivojac, P., Vacic, V., Haynes, C., Cocklin, R. R., Mohan, A., Heyen, J. W., Goebl, M. G., and Iakoucheva, L. M. (2010) Identification, analysis, and prediction of protein ubiquitination sites. *Proteins* **78,** 365–380
6. Finkelstein, R. R., and Lynch, T. J. (2000) The *Arabidopsis* abscisic acid response gene *ABI5* encodes a basic leucine zipper transcription factor. *Plant Cell* **12,** 599–609
7. Lopez-Molina, L., Mongrand, S., and Chua, N. H. (2001) A post-germination developmental arrest checkpoint is mediated by abscisic acid and requires the ABI5 transcription factor in *Arabidopsis*. *Proc. Natl. Acad. Sci. U.S.A.* **98,** 4782–4787
8. Brocard, I. M., Lynch, T. J., and Finkelstein, R. R. (2002) Regulation and role of the *Arabidopsis* abscisic acid-insensitive 5 gene in abscisic acid, sugar, and stress response. *Plant Physiol.* **129,** 1533–1543
9. Smalle, J., Kurepa, J., Yang P., Emborg, T. J., Babiychuk, E., Kushnir, S., and Vierstra, R. D. (2003) Pleiotropic role of the 26 S proteasome subunit RPN10 in *Arabidopsis* growth and development supports a substrate-specific function in abscisic acid signaling. *Plant Cell* **15,** 965–980
10. Liu, H., and Stone, S. L. (2011) E3 ubiquitin ligases and abscisic acid signaling. *Plant Signal. Behav.* **6,** 344–348
11. Stone, S. L., Williams, L. A., Farmer, L. M., Vierstra, R. D., and Callis, J. (2006) KEEP ON GOING, a RING E3 ligase essential for *Arabidopsis* growth and development, is involved in abscisic acid signaling. *Plant Cell* **18,** 3415–3428
12. Liu, H., and Stone, S. L. (2010) Abscisic acid increases Arabidopsis ABI5 transcription factor levels by promoting KEG E3 ligase self-ubiquitination and proteasomal degradation. *Plant Cell* **22,** 2630–2641
13. Gu, Y., and Innes, R. W. (2011) The KEEP ON GOING protein of Arabidopsis recruits the ENHANCED DISEASE RESISTANCE1 protein to trans-Golgi network/early endosome vesicles. *Plant Physiol.* **155,** 1827–1838
14. Lopez-Molina L., Mongrand S., McLachlin D. T., Chait B. T., and Chua N. H. (2002) ABI5 acts downstream of ABI3 to execute an ABA-dependent growth arrest during germination. *Plant J.* **32,** 317–328
15. Lopez-Molina, L., Mongrand, S., Kinoshita, N., and Chua, N. H. (2003) AFP is a novel negative regulator of ABA signaling that promotes ABI5 protein degradation. *Genes Dev.* **17,** 410–418
16. Nakai, K., Horton, P. (1999) PSORT, a program for detecting sorting signals in proteins and predicting their subcellular localization. *Trends Biochem. Sci.* **24,** 34–36
17. Thompson, J. D., Gibson, T. J., Plewniak, F., Jeanmougin, F., and Higgins, D. G. (1997) The CLUSTAL_X windows interface, flexible strategies for multiple sequence alignment aided by quality analysis tools. *Nucleic Acids Res.* **25,** 4876–4882
18. Lu, Q., Tang, X., Tian, G., Wang, F., Liu, K., Nguyen, V., Kohalmi, S. E., Keller, W. A., Tsang, E. W., Harada, J. J., Rothstein, S. J., and Cui, Y. (2010) *Arabidopsis* homolog of the yeast TREX-2 mRNA export complex, components and anchoring nucleoporin. *Plant J.* **61,** 259–270
19. Alonso, J. M., Stepanova, A. N., Leisse, T. J., Kim, C. J., Chen, H., Shinn, P., Stevenson, D. K., Zimmerman, J., Barajas, P., Cheuk, R., Gadrinab, C., Heller, C., Jeske, A., Koesema, E., Meyers, C. C., Parker, H., Prednis, L., Ansari, Y., Choy, N., Deen, H., Geralt, M., Hazari, N., Hom, E., Karnes, M., Mulholland, C., Ndubaku, R., Schmidt, I., Guzman, P., Aguilar-Henonin, L., Schmid, M., Weigel, D., Carter, D. E., Marchand, T., Risseeuw, E., Brogden, D., Zeko, A., Crosby, W. L., Berry, C. C., and Ecker, J. R. (2003) Genome-wide insertional mutagenesis of *Arabidopsis thaliana*. *Science* **301,** 653–657
20. Sparkes, I. A., Runions, J., Kearns, A., and Hawes, C. (2006) Rapid, transient expression of fluorescent fusion proteins in tobacco plants and generation of stably transformed plants. *Nat. Protoc.* **1,** 2019–2025
21. Earley, K. W., Haag, J. R., Pontes, O., Opper, K., Juehne, T., Song, K., and Pikaard, C. S. (2006) Gateway-compatible vectors for plant functional genomics and proteomics. *Plant J.* **45,** 616–629
22. Clough, S. J., and Bent, A. F. (1998) Floral dip, a simplified method for *Agrobacterium*-mediated transformation of *Arabidopsis thaliana*. *Plant J.* **16,** 735–743
23. Wang, F., Zhu, D., Huang, X., Li, S., Gong, Y., Yao, Q., Fu, X., Fan, L. M., and Deng, X. W. (2009) Biochemical insights on degradation of *Arabidopsis* DELLA proteins gained from a cell-free assay system. *Plant Cell* **21,** 2378–2390
24. Sedgwick, S. G., Smerdon, S. J. (1999) The ankyrin repeat, a diversity of interactions on a common structural framework. *Trends Biochem. Sci.* **24,** 311–316
25. Finkelstein, R., Gampala, S. S., Lynch, T. J., Thomas, T. L., and Rock, C. D. (2005) Redundant and distinct functions of the ABA response loci ABA-INSENSITIVE(ABI)5 and ABRE-BINDING FACTOR (ABF)3. *Plant Mol. Biol.* **59,** 253–267
26. Kim, S. Y., Ma, J., Perret, P., Li, Z., and Thomas, T. L. (2002) *Arabidopsis* ABI5 subfamily members have distinct DNA-binding and transcriptional activities. *Plant Physiol.* **130,** 688–697

27. Bensmihen, S., Rippa, S., Lambert, G., Jublot, D., Pautot, V., Granier, F., Giraudat, J., and Parcy, F. (2002) The homologous ABI5 and EEL transcription factors function antagonistically to fine-tune gene expression during late embryogenesis. *Plant Cell* **14,** 1391–1403
28. Meier, I., and Somers, D. E. (2011) Regulation of nucleocytoplasmic trafficking in plants. *Curr. Opin. Plant Biol.* **14,** 538–546
29. Suo, Y., and Miernyk, J. A. (2004) Regulation of nucleocytoplasmic localizatioin of the atDjC6 chaperone protein. *Protoplasma* **224,** 79–89
30. Igarashi, D., Ishida, S., Fukazawa, J., and Takahashi, Y. (2001) 14-3-3 proteins regulate intracellular localization of the bZIP transcriptional activator RSG. *Plant Cell* **13,** 2483–2497
31. Kircher, S., Wellmer, F., Nick, P., Rügner, A., Schäfer, E., and Harter, K. (1999) Nuclear import of the parsley bZIP transcription factor CPRF2 is regulated by phytochrome photoreceptors. *J. Cell Biol.* **144,** 201–211
32. Lee, J. H., Yoon, H. J., Terzaghi, W., Martinez, C., Dai, M., Li, J., Byun, M. O., and Deng, X. W. (2010) DWA1 and DWA2, two Arabidopsis DWD protein components of CUL4-based E3 ligases, act together as negative regulators in ABA signal transduction. *Plant Cell* **22,** 1716–1732